JACS
JOURNAL OF THE AMERICAN CHEMICAL SOCIETY

Article

pubs.acs.org/JACS

Theoretical and Experimental Investigations of Circular Dichroism and Absolute Configuration Determination of Chiral Anthracene Photodimers

Ayako Wakai, Hiroki Fukasawa, Cheng Yang, Tadashi Mori,* and Yoshihisa Inoue*

Department of Applied Chemistry, Graduate School of Engineering, Osaka University, 2-1 Yamada-oka, Suita, Osaka 565-0871, Japan

Supporting Information

ABSTRACT: Substituted anthracenes photodimerize to stereoisomeric [4 + 4] cyclodimers, some of which are inherently chiral. Recent supramolecular photochirogenic studies enabled the efficient preparation of specific stereoisomers, the absolute configurations of which should reflect the chiral environment of supramolecular host or scaffold employed but have not been determined, hindering detailed mechanistic elucidation and further host/scaffold design. In this study, we performed the combined experimental and state-of-the-art theoretical analyses of the circular dichroism spectra of chiral cyclodimers of 2-anthracenecarboxylic and 2,6-anthracenedicarboxylic acids to reveal the configurational and molecular orbital origin of the Cotton effects observed, and unambiguously determined the absolute configurations of these chiral cyclodimers. The present results allow us to directly correlate the enantiotopic face-selectivity upon photocyclodimerization with the absolute configuration of the cyclodimer derived therefrom and also to precisely elucidate the chiral arrangement of two cyclodimerizing anthracenes.

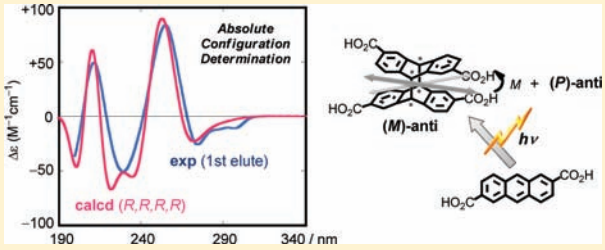

INTRODUCTION

Photocyclodimerization of anthracene to [4 + 4] cyclodimer, 5,6,11,12-tetrahydro-5,12:6,11-bis([1,2]benzeno)dibenzo[*a*,*e*]-[8]annulene, is one of the most comprehended photochemical reactions.[1,2] Thus, the photocyclodimerization behavior of various anthracene derivatives has been well characterized and often employed as a key tool for photochemically constructing and controlling various nano- and biomaterials.[3,4] Recent supramolecular approaches significantly improved the photocyclodimerization efficiency through the substrate preorganization by cyclodextrins,[5] curcurbit[*n*]urils,[6] hydrophobic nanocapsules,[7] organogel systems,[8] DNA scaffolds,[9] and proteins such as serum albumins[10,11] and prefoldin.[12] The photocyclodimerization of unsymmetrically modified anthracene derivatives, such as 1- and 2-substituted anthracenes, affords anti/syn pairs of head-to-tail (HT) and head-to-head (HH) cyclodimers, two of which (i.e., *syn*-HT and *anti*-HH isomers) are chiral.[13,14] More recently, the photocyclodimerization of 2-anthracenecarboxylic acid (**AC**) was broadly exploited by us[15−17] and others[8,18] as a benchmark reaction for evaluating the photochirogenic ability of chiral supramolecular system, because the enantiomeric excess of chiral **AC** dimer (**dAC**) produced is a critical function of host structure, occupancy, and binding mode. Nevertheless, the absolute configurations of enantiomeric **dAC**s have not been determined experimentally by X-ray crystallography or theoretically by quantum chemical calculations. This obviously holds back our comprehensive understanding and in-depth discussion of the chirogenic interactions of **AC** molecules in supramolecular environment in the ground and excited states.

From the structural point of view, the paired butterfly shaped anthracene dimers are of particular interest as conformationally frozen dual [2.2]orthocyclophanes with four aromatic planes spatially arranged at specific angles and distances, as is the case in [2.2]paracyclophanes,[19] multidecker cyclophanes,[20,21] and triptycenes.[22,23]

Recent theoretical advances in quantum chemical calculation methods, particularly the time-dependent density functional theory (TD-DFT),[24,25] allow us to unambiguously determine the absolute configurations of various chiral molecules by comparing the theoretical versus experimental electronic circular dichroism (CD) spectra.[26,27] Despite the numerous apparently successful results reported in the literature,[28−30] the TD-DFT calculation is known to be very sensitive to the functionals employed.[31] Nevertheless, the TD-DFT is a method of choice in many cases simply because the efficiency overrides the deficiencies in general. However, when the system is ionic, charge transfer, Rydberg, and multichromophoric in nature, the TD-DFT often fails to properly predict the (spectroscopic) properties even with small molecules such as paracyclophane.[32] Therefore, a complementary approach with several theoretical methods is mandatory for a reliable determination of the absolute configurations of chiral **dAC**s, possessing four quasi-equivalent aromatic systems. In this combined experimental and theoretical study to elucidate the chiroptical properties and the absolute configurations[33] of chiral **dAC**s, we employed a stepwise approach, starting with the chiral cyclodimer of 2,6-

Received: January 17, 2012
Published: February 23, 2012

dx.doi.org/10.1021/ja300522y | *J. Am. Chem. Soc.* 2012, 134, 4990−4997

Scheme 1. Photocyclodimerization of 2,6-Anthracenedicarboxylic Acid (AD)[a]

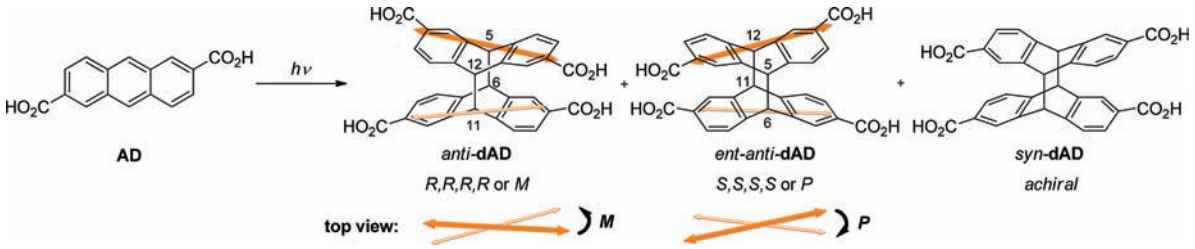

[a]Note that the "*P*/*M*" chirality is defined as the right- or left-handed screw arrangement of the longer axes of two former **AD**.

anthracenedicarboxylic acid (**AD**) with four of exactly the same chromophores and then proceeding to chiral **dAC**s with quasi-equivalent four chromophores.

RESULTS AND DISCUSSION

Experimental Spectra of Chiral AD Dimer. Although **AD** is a known compound[34,35] and is expected to cyclodimerize upon irradiation, its photochemistry has not been reported in the literature. In the present study, we found that the photocyclodimerization of **AD** smoothly proceeds indeed in a neutral solution (buffered, pH = 7) upon irradiation at >320 nm to give a nearly 1:1 mixture of two stereoisomeric cyclodimers (**dAD**), that is, achiral *syn*- and chiral *anti*-isomers (Scheme 1), which were separated by repeated washing by acetonitrile, and the *anti*-isomer thus obtained was subjected to preparative HLPC on a chiral column (Daicel OJ-RH) to give a pair of enantiopure *anti*-**dAD** and *ent-anti*-**dAD**, which were tentatively termed according to the elution order under the condition employed; see the Supporting Information for details. With the enantiopure *anti*-**dAD** (first eluted) sample in hand, we proceeded to the combined theoretical and experimental studies of its chiroptical properties and absolute configuration.

In general, experimental spectra measured in less-polar solvents are favored for the direct comparison with theoretical ones, as one can circumvent the consideration of complicated solvation issues. However, *anti*-**dAD** in its protonated form turned out to be scarcely soluble in less-polar solvents, such as pentane, methylcyclohexane, diethyl ether, and THF, and only slightly soluble in acetonitrile to give a slurry, with which we could manage to record the CD spectrum (but not the UV spectrum due to the severe scattering of incident light). The solubility of *anti*-**dAD** was greatly improved in aqueous (alkaline) media, where *anti*-**dAD** is in its anionic tetracarboxylate form. Hence, an aqueous KOH (10 mM) solution of *anti*-**dAD** was employed for measuring UV and CD spectra (Figure 1, black lines).

As can be seen from the UV and CD spectra shown in Figure 1, there are four apparent bands labeled A, B, C, and D from the low-energy end, which are tentatively assigned to the ^1L_b, ^1L_a, ^1B_b, and ^1B_a transitions, respectively, according to the Platt notation.[36] The apparently coupled, that is, negative−positive−negative−positive Cotton effects were observed for the first-eluted enantiomer of *anti*-**dAD** (Figure 1, right). The anisotropy (g) factors at the ^1L_b and ^1L_a transitions are fairly large as allowed $\pi-\pi^*$ transitions, reaching $5-6 \times 10^{-3}$ (see Figure S4 in the Supporting Information).[37] Although the accurate ellipticities could not be determined in acetonitrile due to the turbidness, the overall CD profiles of neutral *anti*-**dAD** in acetonitrile and *anti*-**dAD** anion in aqueous solution surprisingly resemble each other in shape and intensity, only accompanying slight band shifts. This means that the carboxyl moiety of **dAD** is not significantly incorporated into the aromatic π system and the apparently large change from the neutral carboxylic acid to anionic carboxylate does not greatly influence the $\pi-\pi^*$ transitions, which is compatible with the result of theoretical calculations that the effect of carboxyl moieties on the overall CD spectra of anthracene dimers is rather small (vide infra). In addition, the effective solvation to the carboxylate anions may moderate the influence of deprotonation from **dAD**.

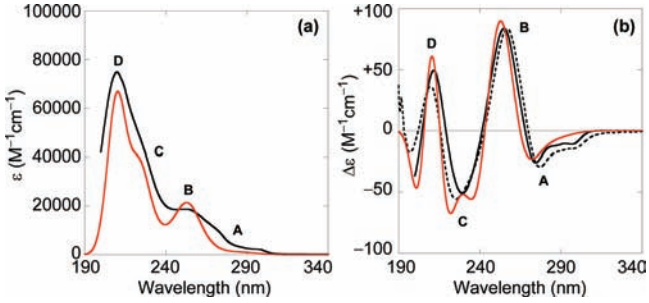

Figure 1. Comparison of the experimental and theoretical UV (left) and CD (right) spectra of the first-eluted enantiomer of *anti*-**dAD** on chiral HPLC (Daicel OJ-RH column). Red: Theoretical spectra calculated for (*R*,*R*,*R*,*R*)- or (*M*)-*anti*-**dAD** at the RI-CC2/TZVPP level. Black: Experimental spectra in aqueous 10 mM KOH solution (solid line) and in acetonitrile (dotted, CD only) at 25 °C. Note that the solubility of *anti*-**dAD** is very limited in acetonitrile, and hence the CD spectrum in this solvent was recorded as a suspension. Consequently, the CD intensity was normalized at the extrema at 255 nm for acetonitrile solution and 257 nm for aqueous solution.

Theoretical Spectra of Chiral AD Dimer. Benzoic acid is energetically most stable when the carboxyl group is coplanar to the benzene ring due to the most effective conjugation, while the carboxyl substituent can be either *s-cis* or *s-trans* about the C−C(=O) bond. Possessing four benzoic acid moieties, *anti*-**dAD** can take seven independent conformations altogether: that is, *tttt*, *cttt*, *cctt*, *cttc*, *tctc*, *cctc*, and *cccc*, where *c* and *t* denote *s-cis* and *s-trans*, respectively. All of the seven possible conformers were geometrically optimized at the DFT-D-B97-D/TZVP level[38,39] to give the lowest energy for the *tttt*-conformer illustrated in Figure 2 (the geometries of all possible conformers are shown in the Supporting Information). The relative energies were calculated also at the more accurate SCS-MP2/TZVPP level[40] to double-check the reliability of the DFT method chosen, from which the Boltzmann population of each conformer was computed at the two levels of theory to afford comparable values (Table S1 in the Supporting Information). Energetically, the *s-trans* conformation is slightly favored over

dx.doi.org/10.1021/ja300522y | J. Am. Chem. Soc. 2012, 134, 4990−4997

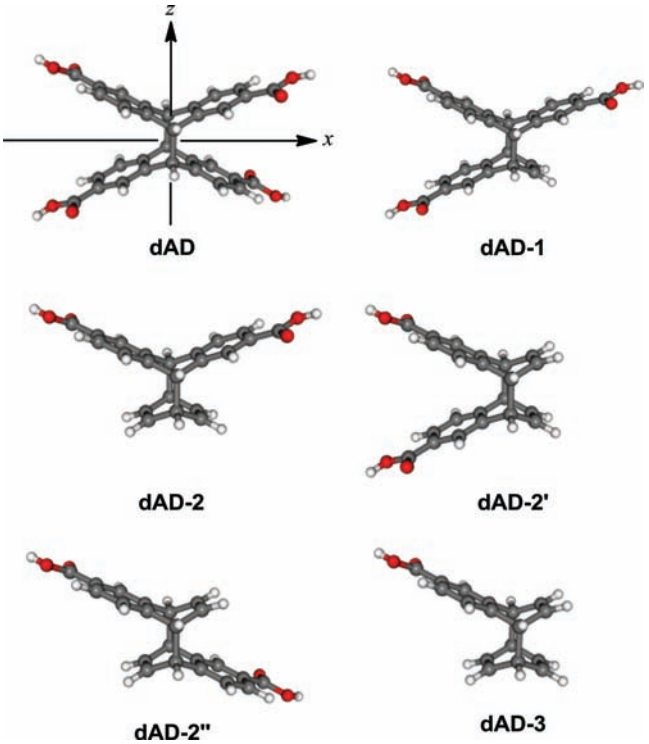

Figure 2. Optimized structures of **dAD-0** (*tttt-anti-***dAD**), and its lower homologues **dAD-1**, **dAD-2**, **dAD-2′**, **dAD-2″**, and **dAD-3** (lacking one to three benzoic acid moiety/ies) at the DFT-D-B97-D/TZVP level.

the *s-cis*, and each *s-cis* introduced leads to a steady increase of 0.2 kcal mol^{-1}. The overall energy difference between the most stable *tttt* and the least stable *cccc* is as low as 0.8 kcal mol^{-1}, and hence all of the seven conformations are expected to be populated appreciably at 25 °C (Table S1).

Interestingly and somewhat fortunately, such differences in conformation turned out not to significantly affect the predicted UV and CD spectra, enabling us to circumvent the tedious conformation issue. Thus, the theoretical UV and CD spectra of these seven conformers, obtained by the linear response approximate coupled cluster calculation[41,42] at the RI-CC2/SV(P) level, were practically superimposable with each other in the ^1L_b and ^1L_a region and only slightly varied in intensity in the ^1B region (Figure S5 in the Supporting Information). Subsequent theoretical calculations with the most and least stable *tttt*- and *cccc*-conformers with the TZVPP basis set revealed that the theoretical UV and CD spectra were qualitatively very close to those obtained with the smaller basis set of SV(P) (Figures S6 and S7 in the Supporting Information). Both of the excitation energies calculated by using the two basis sets were overestimated relative to the experimental values, but the deviation was more pronounced for the smaller basis sets; the shifts required are 0.2 and 0.5 eV for TZVPP and SV(P) basis-sets, respectively. Briefly, the above theoretical studies on the conformational isomer of *anti-***dAD** revealed that altering *s-cis*/*s-trans* conformation of the peripheral carboxyl groups can induce only very small, often negligible, nonessential changes in UV and CD spectra. In this regard, it may be pointed out that the effect of basis-set saturation on the CD (and UV) spectra is larger than that of the conformational variation. Consequently, we will concentrate on the most stable *tttt*-conformer of *anti-***dAD** and discuss the theoretical UV and CD spectra calculated for this specific conformer at the RI-CC2/TZVPP level.

Before discussing the nature of the transitions involved in *anti-***dAD** (meaning the *tttt*-conformer hereafter) and its absolute configuration determination, we want to briefly describe the results of other theoretical treatments (all of the UV and CD spectra calculated by different theoretical methods can be found in Figures S8 and S9 in the Supporting Information). The Pariser−Parr−Pople theory is known to be remarkably accurate in describing many of the low-lying excitations in a wide range of conjugated π systems.[43,44] This method, however, turned out to be completely ineffectual for the current system. We then tested the cost-efficient time-dependent density functional theory (TD-DFT),[45,46] employing a wide range of parametrized and nonparameterized hybrid functionals with different degrees of exact exchange. The results of popular B3-LYP, as well as PBE0, functionals were quite unsatisfactory. The TD-DFT calculation with the BH-LYP functional, which contains as much as 50% of exact exchange, outperformed in reproducing the UV and CD spectra of *anti-***dAD**. The pattern of Cotton effects (signs and relative excitation energies) was well reproduced by this functional, as compared to the experiment, while the relative intensities of bands B and C were not properly reproduced. A recently introduced double-hybrid density functional theory (B2-PLYP method),[47] which is generally superior to the standard hybrid GGA methods, was also tested. The results were quantitatively analogous to those obtained with the TD-DFT with the BH-LYP functional. It is to note that a large portion of exact exchange (53%) is also involved in the B2-PLYP method. Such a large amount of exact exchange in BH-LYP and B2-PLYP methods seems to diminish the problems related to the self-interaction error, and thus outperform in reproducing the UV and CD spectra of *anti-***dAD**. The long-range separated functionals such as LC-B3LYP and CAM-BLYP may be a potential alternative to better describe the electronic transitions for certain difficult cases,[48] but further assessment of such methods on the present system was beyond the scope of our study. Although we will eventually employ the results of the more accurate RI-CC2/TZVPP calculations in the following discussion, the BH-LYP and B2-PLYP methods may be of reasonable choice when the system in mind is relatively large and the expensive methods such as the RI-CC2 calculation become practically not feasible. The fact that the qualitatively parallel outcomes were gained with different density functionals further made the assignment of absolute configuration convincing. It should be noted, however, that the theoretical UV and CD spectra calculated for the tetracarboxylate anion of *anti-***dAD** at the RI-CC2/TZVPP level totally failed to reproduce the experimental spectra measured in aqueous alkaline solutions (Figure S10 in the Supporting Information). Probably, the calculation of such an anionic species was not suitable in our calculations, which essentially ignore the effect of solvation. Rather, the theoretical spectra obtained for the neutral tetracarboxylic acid better reproduced the experimental ones obtained in both acetonitrile and aqueous solutions. Similar observations have also recently appeared in the literature.[49]

Figure 1 compares the theoretical UV and CD spectra calculated at the RI-CC2/TZVPP level with the experimental spectra. With this single reference time-dependent approximate coupled cluster theory, all of the four bands (A−D) are reproduced quite nicely both in UV and in CD spectra. On the

dx.doi.org/10.1021/ja300522y | *J. Am. Chem. Soc.* 2012, 134, 4990−4997

basis of the excellent agreement of the theoretical and experimental CD spectra, we can unambiguously assign the absolute configuration of the first-eluted enantiomer of *anti*-**dAD** as "5*R*,6*R*,11*R*,12*R*", or simply "*M*" chirality due to the left-handed (minus) screw arrangement of the longer axes of two former **AD** (each axis passing through the two carboxylic acid substituents). A closer examination revealed a slight difference in band C, where two negative extrema are found in the calculated CD spectrum, while an apparently single band appears in the experiment. Theoretically, the situation is more complicated, each band being composed of more than two transitions as shown in the bar spectrum of the rotatory strengths calculated for *anti*-**dAD** (Figure 3). The properties of each transition, such as excitation energy, oscillator and rotatory strength, and band configuration, are listed in Table 1 (see also Table S2 in the Supporting Information for further details). Interestingly, the transitions contributed to the observed CD spectrum are either *y*- or *z*-axis polarized, both of which are perpendicular to the long axis of *anti*-**dAD** molecule. The transitions along the long *x*-axis bear the same b-symmetry, but are much smaller in CD intensity and almost negligible in the overall CD spectrum, while the a-symmetry transitions are forbidden.

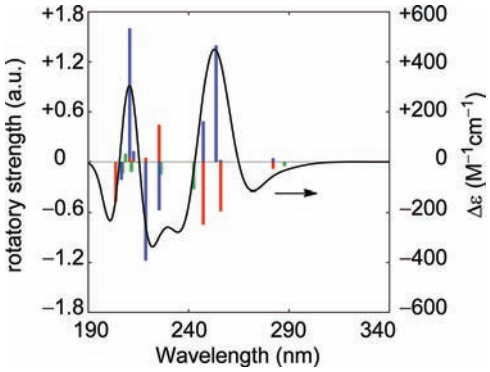

Figure 3. Bar representation of the rotatory strength of the most abundant *tttt*-conformer of *anti*-**dAD** calculated at the RI-CC2/TZVPP level. Red: Transitions of b1 symmetry (*z*-axis). Green: Transitions of b2 symmetry (*y*-axis). Blue: Transitions of b3 symmetry (*x*-axis). Solid line is the theoretical CD spectrum of *tttt-anti*-**dAD** for comparison.

Analyses of the configuration of transitions (Table 1) and the molecular orbitals (MOs) involved in each transition (Figure 4) provide additional insights into the nature of the Cotton effects observed for the anthracene dimer. Most of the bands are composed of more than two transitions involving different pairs of MOs, meaning that the analysis of the CD spectrum of *anti*-**dAD** is not straightforward. This is one of the reasons why the standard TD-DFT method, and the P−P−P method as well, failed to reproduce the experimental CD spectra. It is also important to note that as much as 11−15% of doubles contribute to the excited-state wave functions of *anti*-**dAD**, augmenting the complexity of the *anti*-**dAD** transitions. Borrowing the notation for benzene's MOs, we may categorize the MOs involved in these major transitions into bonding and antibonding, which correspond to the π_2/π_3 and π_4/π_5 orbitals of benzene molecule, respectively. Orbital 33a is distributed over the whole molecule along the bonding directions (probably σ-type), while orbital 33b2 is located mostly on the carbonyl moiety. These orbitals, however, are not involved in the major transitions of the CD spectrum shown in Figure 3 or Table 1. All of the transitions are basically $\pi-\pi^*$ in nature, but become complex due to the significant interactions between the chromophores. It is noteworthy that the transitions associated with the carbonyl moieties are essentially not involved in these transitions. The fact that the theoretical CD spectrum of *anti*-**dAD** is insensitive to the *s-cis*/*s-trans* conformation of the carboxyl groups supports the conclusion that the carboxyl moieties in **dAD** do not directly affect the observed CD, but simply lower the energy of each MO. This is also in line with the fact that the neutral and anionic forms of *anti*-**dAD** exhibit essentially the same CD spectra in acetonitrile and aqueous solutions.

The CD spectrum of *anti*-**dAD** was further studied in detail by using model systems shown in Figure 2. Thus, a series of lower homologues **dAD-*n*** (n = 0−3), generated by systematically removing n unit(s) of the benzoic acid moieties from the most stable conformer *tttt-anti*-**dAD** (i.e., **dAD-0**), were subjected to the quantum chemical calculations. The geometries of these homologues were optimized at the DFT-D-B97-D/TZVP level, and the CD spectra were calculated at the RI-CC2/TZVPP level; see Figure S11 in the Supporting Information for individual UV and CD spectra of these homologues. Naturally, the calculated spectra of the homologues differed mutually and also from that of parent **dAD-0**.

Table 1. Properties of Selected Transitions and Their Contributions to the CD Spectrum of *tttt-anti*-dAD Calculated at the RI-CC2/TZVPP Level[a]

state	transition energy	oscillator strength	rotatory strength	contributions[b]
2B1	4.839	0.049	−0.587	35b2−35b3 (49%), 35b2−36b3 (14%), 35a−35b1 (10%), 34b2−35b3 (10%)
3B3	5.087	0.459	+1.397	35b2−35b1 (67%), 35a−35b3 (12%)
4B3	5.214	0.050	+0.486	34a−35b3 (85%)
3B2	5.312	0.049	−0.328	35b2−36a (36%), 35a−36b2 (20%), 34b3−35b1 (14%), 33b1−35b3 (11%)
4B1	5.433	0.141	−0.745	34a−35b1 (81%)
5B3	5.702	0.278	−0.573	35a−35b3 (50%), 34b2−35b1 (20%), 35b2−36b1 (10%)
6B1	5.713	0.325	+0.445	35b2−36b3 (52%), 34b2−35b3 (33%)
7B3	5.871	0.265	−1.176	34b3−36a (48%), 34b2−35b1 (12%), 33b3−36a (11%)
8B3	6.087	0.865	+1.603	34b3−36a (32%), 33b3−36a (29%), 34b2−35b1 (28%)
10B3	6.288	0.087	−0.309	34b1−36b2 (84%)
10B1	6.340	0.077	−0.468	33b1−36a (63%), 33b3−36b2 (14%)

[a]The transitions of rotatory strength > 0.3 are selected. Transition energies are in electronvolt. The oscillator and rotatory strengths are in atomic unit. [b]The configurations that contributed more than 10% are selected.

dx.doi.org/10.1021/ja300522y | *J. Am. Chem. Soc.* 2012, 134, 4990−4997

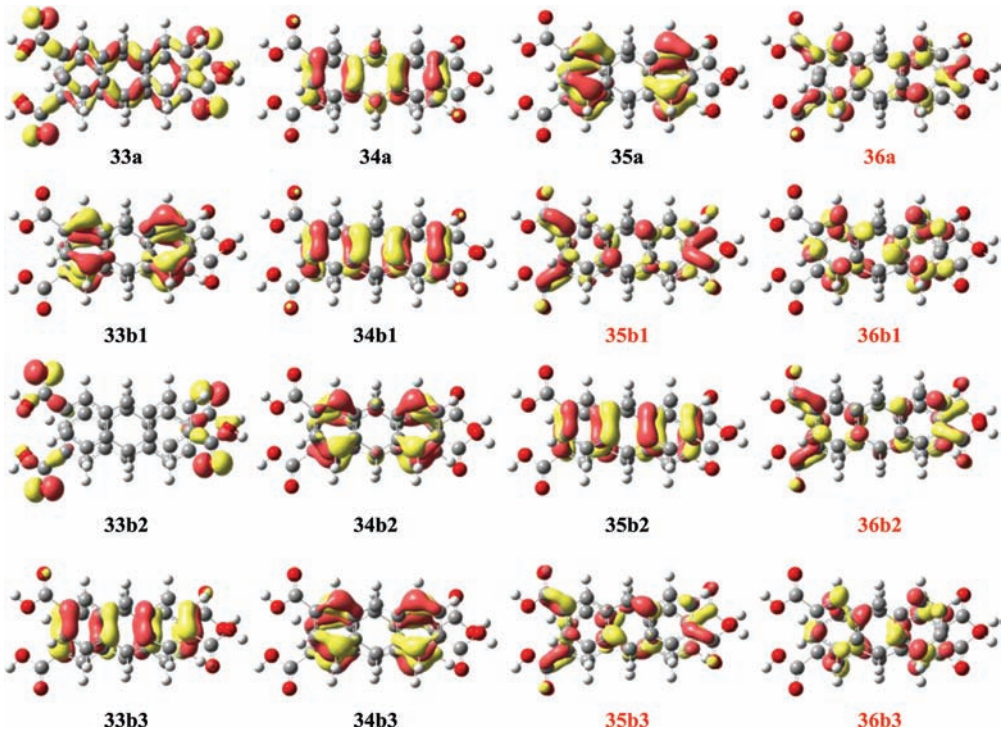

Figure 4. Molecular orbitals associated with the main transitions found in the CD spectrum of *anti*-**dAD** shown in Figure 3 and Table 1; most of the MOs are of single-noded π_2/π_3 or double-noded π_4/π_5 type in the conventional notation used for benzene. The labels for the occupied and the virtual orbitals are indicated in black and red, respectively.

Remarkably, a summation of the CD spectra calculated for **dAD-2**, **dAD-2′**, and **dAD-2″** showed reasonable agreement at the low-energy bands A–C with that of **dAD-0** (Figure 5a),

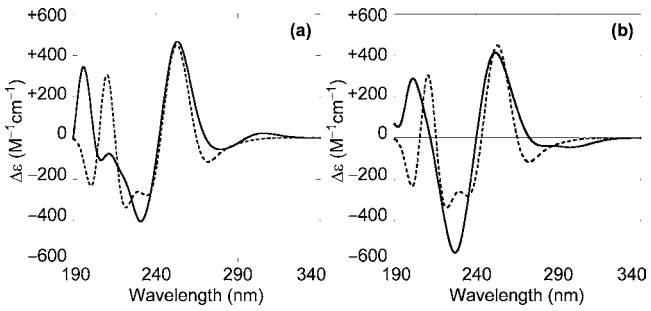

Figure 5. Comparison of the CD spectrum calculated for **dAD-0** (- - -) with (a) a sum spectrum of **dAD-2**, **dAD-2′**, and **dAD-2″** (—) and (b) that of **dAD-1** and **dAD-3** (solid) at the RI-CC2/TZVPP level.

which comprises all interacting four benzoic acids. For a symmetry reason, the pattern of Cotton effect is qualitatively analogous to those of **dAD-2** and **dAD-2″**, but inverted in sign for **dAD-2′**. The latter species bears symmetry along the long axis of **dAD**, while the former two do so along the shorter axes. Thus, mutual cancellation leads to the first negative, second positive, and third negative Cotton effects at bands A–C. The less sufficient matching at the high-energy band D may be (at least in part) due to an improper estimation of the excitation energies in these models. Considering the fact that simple TD-DFT methods were not enough to reproduce the CD spectra of anthracene dimers and the coupled cluster calculations were needed, we should emphasize that the observed transitions in the anthracene dimers were described sufficiently by a combination of the transitions provided by the interactions between each pair of benzoic acids. It is also important to note that most of the important features of the observed CD spectrum of *anti*-**dAD** were nicely reproduced by combining the theoretical spectra of mono- and trisubstituted systems, **dAD-1** and **dAD-3** (Figure 5b).

Theoretical Spectra of Chiral AC Dimers. The photocyclodimerization of 2-anthracenecarboxylic acid (**AC**), affording the anti/syn pairs of HT and HH dimers (Scheme 2), has been a target of intensive studies in recent years[15−18] as a benchmark photochirogenic reaction to control the stereochemical outcomes, that is, the anti/syn, HT/HH, and in particular the enantiomer ratios. As a consequence of the nonequivalent chromophores incorporated and the lower symmetry (C_2), theoretically calculating the CD spectra of chiral **AC** dimers, that is, *syn*-HT (**dAC**) and *anti*-HH (**dAC′**), is obviously more challenging.

We first obtained the optimized geometries of the two chiral **dAC**s at the DFT-D-B97-D/TZVP level. In these calculations, we considered only the *s-trans* conformation of the carboxylic acid moieties, as this part did not appreciably affect the overall CD spectrum in the **dAD** cases (vide supra). The theoretical CD spectra were calculated for (*M*)- or (5*S*,6*S*,11*R*,12*R*)-**dAC** and (*P*)- or (5*R*,6*S*,11*R*,12*S*)-**dAC′** (Scheme 2) at the RI-CC2/TZVPP level. Note that the "*P*/*M*" chirality is defined as the right- or left-handed screw arrangement of the longer axes of two former **AC** (each axis passing through the carboxylic acid substituent; see Scheme 2).

Figure 6 compares the experimental and theoretical CD spectra of **dAC** and of **dAC′**. Interestingly, **dAC**, lacking two carboxylic acid moieties at the most distant positions, showed a CD spectrum very similar in pattern and relative intensity to that obtained for *anti*-**dAD** (compare Figure 6a with Figure 1b). The CD spectrum of **dAC** also resembles that of **dAD-2″** (except the band D) (Figure 2 and Figure S11b in the

dx.doi.org/10.1021/ja300522y | *J. Am. Chem. Soc.* 2012, 134, 4990−4997

Scheme 2. Photocyclodimerization of 2-Anthracenecarboxylic Acid (AC)[a]

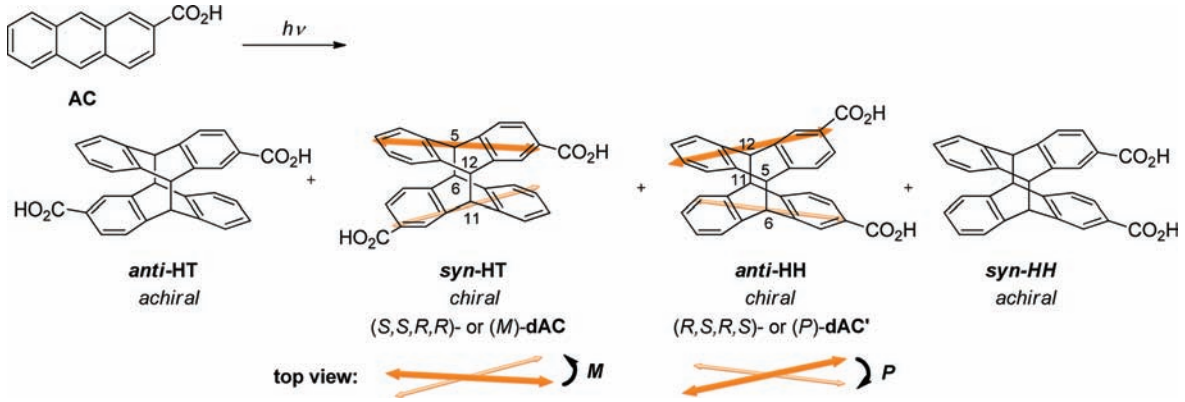

[a]Only one of the enantiomers is shown for clarity for chiral *syn*-HT (**dAC**) and *anti*-HH (**dAC′**) dimers.

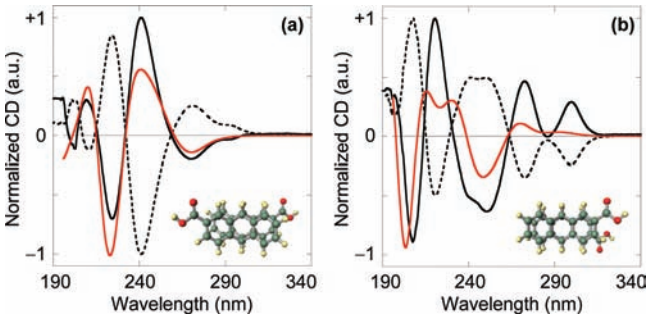

Figure 6. Comparison of the experimental and theoretical CD spectra of *syn*-HT dimer **dAC** (left) and *anti*-HH dimer **dAC′** (right); insets show the optimized geometries used for calculations. The experimental CD spectra of the first and second elutes (solid and dotted black lines, respectively) from a tandem column of ODS and Daicel OJ-RH were recorded in methanol, and the rotatory strengths were normalized at the strongest peak. The theoretical spectra (red lines) were calculated at the RI-CC2/TZVPP//DFT-D-B97-D/TZVP level for (*M*)- or (5*S*,6*S*,11*R*,12*R*)-**dAC** (left) and (*P*)- or (5*R*,6*S*,11*R*,12*S*)-**dAC′** (right).

Supporting Information), despite missing two aromatic rings, suggesting the *syn*-HT arrangement of two benzoic acid moieties is essential and sufficient to develop the Cotton effect pattern observed for **dAC** (and **dAD**). Furthermore, the CD spectra of **dAC** and **dAD** share a common feature of the apparent split of the low-energy band A. From a direct comparison of the theoretical versus experimental CD spectra (Figure 6a), we can unambiguously assign the absolute configuration of the first-eluted enantiomer of **dAC** as "*M*" or "5*S*,6*S*,11*R*,12*R*".

The theoretical and experimental CD spectra of *anti*-HH dimer **dAC′** exhibited qualitatively the same alternating patterns but significant deviations in relative intensity (Figure 6b). It is important to note that the experimental CD spectrum of **dAC′**, with bands A and B being fully or partially split, obviously differs from those of **dAC** and **dAD** but rather resembles that of **dAD-2′** (Figure 2 and Figure S11b in the Supporting Information), in which two facing benzoic acid moieties are removed from parent **dAD-0**. Although the relative CD intensities were less properly reproduced in the theoretical spectrum than the **dAD** and **dAC** cases, the signs and alternating pattern of the experimental Cotton effects (except the one at ca. 230 nm) were reproduced satisfactorily. Therefore, the absolute configuration of the first-eluted enantiomer of **dAC′** was determined as "*P*" or "5*R*,6*S*,11*R*,12*S*". The exact origin of the larger deviations in relative intensity is not clear at present and remains to be elucidated.

CONCLUSIONS

In this combined theoretical and experimental CD spectral study, we have determined for the first time the absolute configurations of chiral anthracene photodimers **dAD**, **dAC**, and **dAC′**, in which four equivalent or quasi-equivalent aromatic systems are located in close proximities, making the theoretical calculation more demanding and complex. Thus, the first fractions of chiral **dAD**, **dAC**, and **dAC′**, eluted from chiral HPLC under the conditions employed, were unequivocally assigned to (5*R*,6*R*,11*R*,12*R*)-**dAD**, (5*S*,6*S*,11*R*,12*R*)-**dAC**, and (5*R*,6*S*,11*R*,12*S*)-**dAC′**. The screw-shaped molecular geometry allows us to truncate the redundant absolute configurations to (*M*)-**dAD**, (*M*)-**dAC**, and (*P*)-**dAC′**.

The detailed analysis of the theoretical predictions revealed that most of the important Cotton effects observed in the (apparently) complicated and severely coupled CD spectrum of **dAD** are aligned along the shorter axis (perpendicular to *x*-axis) of the molecule, while the transitions along the long *x*-axis are much smaller and almost negligible in the observed CD. The MO analyses revealed that the contribution of the carboxyl moieties to the CD spectrum is insignificant. Most surprisingly, most of the important features of the observed CD spectrum of **dAD** can be nicely reproduced by simply summing up the CD spectra calculated for the lower homologues composed of two benzoic acids.

The present elucidation of the absolute configurations of chiral anthracene dimers will enable us not only to precisely analyze the enantio- and diastereotopic face selectivities of photoreactive substrates in chiral supramolecular environment, but also to expand the range of photosubstrate and further promote the research in molecular and supramolecular chiral photochemistry through application of the present methodologies to other photochirogenic systems. Our immediate target will be the photocyclodimerization of **AD** in chiral supramolecular environment.

COMPUTATIONAL METHODS

All calculations were performed on Linux-PCs using the TURBOMOLE 6.2 program suite.[50] All conformers of **dAD** and **dAC** were optimized at the DFT-D-B97-D/TZVP level (H, [3s1p], C/O,

dx.doi.org/10.1021/ja300522y | *J. Am. Chem. Soc.* 2012, 134, 4990−4997

[5s3p1d]) with numerical quadrature grid m4, with an appropriate symmetry option (D_2, C_2, or C_1).[38,39] Subsequent single-point energy calculations were performed at the most reliable SCS-MP2 level with a basis set of TZVPP quality (H, [3s2p1d], C/O, [5s3p2d1f]).[40] The resolution of identity (RI) approximation was employed in all DFT-D and SCS-MP2 calculations, and the corresponding auxiliary basis sets were taken from the TURBOMOLE basis-set library. All excited-state calculations were performed with the optimized ground-state geometries and were calculated by the resolution of the identity, time-dependent approximate coupled cluster (RI-CC2) method with the basis-sets of SV(P) or TZVPP quality.[41,42] The spectra were also simulated on the basis of time-dependent density functional theory (TD-DFT) employing the various hybrid functionals such as BH-LYP, PBE0, or B3-LYP, as well as by the time-dependent double-hybrid density functional theory (B2-PLYP),[47] with the TZVP basis-set. The UV and CD spectra were simulated by overlapping Gaussian functions for each transition from the length-gauge representations where the width of the band at 1/e height is fixed at 0.4 eV. Because of the systematic errors of the theoretical transition energies as compared to the experimental ones, the spectra were uniformly red-shifted by 0.2 eV, unless otherwise stated. The calculated band intensities were larger than the experimental counterparts. This is frequently observed in the theoretical calculations and explained as a result of the neglect of averaging over the vibrational wave functions. Thus, the theoretical UV and CD spectra were scaled to one-half and one-fifth, respectively, to match the experimental spectra. More details are described in the Supporting Information.

■ ASSOCIATED CONTENT

Supporting Information

Details of preparation, enantiomer separation, spectroscopic data, and theoretical calculations for **dAD** and **dAC**s. This material is available free of charge via the Internet at http://pubs.acs.org.

■ AUTHOR INFORMATION

Corresponding Author

tmori@chem.eng.osaka-u.ac.jp

Notes

The authors declare no competing financial interest.

■ ACKNOWLEDGMENTS

Financial support of this research by a Grant-in-Aid for Scientific Research (nos. 23350018 and 21245011) from JSPS, the Mitsubishi Chemical Corp. Fund, the Sumitomo Foundation, the Shorai Foundation for Science and Technology, and the Kurata Memorial Hitachi Science and Technology Foundation is gratefully acknowledged.

■ REFERENCES

(1) Becker, H.-D. *Chem. Rev.* **1993**, *93*, 145−172.
(2) Zade, S. S.; Zamoshchik, N.; Reddy, A. R.; Fridman-Marueli, G.; Sheberla, D.; Bendikov, M. *J. Am. Chem. Soc.* **2011**, *133*, 10803−10816.
(3) Bouas-Laurent, H.; Desvergne, J.-P.; Castellan, A.; Lapouyade, R. *Chem. Soc. Rev.* **2000**, *29*, 43−55.
(4) Bouas-Laurent, H.; Desvergne, J.-P.; Castellan, A.; Lapouyade, R. *Chem. Soc. Rev.* **2001**, *30*, 248−263.
(5) Nakamura, A.; Inoue, Y. *J. Am. Chem. Soc.* **2003**, *125*, 966−972.
(6) Yang, C.; Mori, T.; Origane, Y.; Ko, Y. H.; Selvapalam, N.; Kim, K.; Inoue, Y. *J. Am. Chem. Soc.* **2008**, *130*, 8574−8575.
(7) Kaanumalle, L. S.; Gibb, C. L. D.; Gibb, B. C.; Ramamurthy, V. *J. Am. Chem. Soc.* **2005**, *127*, 3674−3675.
(8) Dawn, A.; Fujita, N.; Haraguchi, S.; Sada, K.; Shinkai, S. *Chem. Commun.* **2009**, 2100−2102.
(9) Ihara, T.; Fujii, T.; Mukae, M.; Kitamura, Y.; Jyo, A. *J. Am. Chem. Soc.* **2004**, *126*, 8880−8881.
(10) Nishijima, M.; Wada, T.; Mori, T.; Pace, T. C. S.; Bohne, C.; Inoue, Y. *J. Am. Chem. Soc.* **2007**, *129*, 3478−3479.
(11) Nishijima, M.; Pace, T. C. S.; Nakamura, A.; Mori, T.; Wada, T.; Bohne, C.; Inoue, Y. *J. Org. Chem.* **2007**, *72*, 2707−2715.
(12) Bando, K.; Zako, T.; Sakono, M.; Maeda, M.; Wada, T.; Nishijima, M.; Fukuhara, G.; Yang, C.; Mori, T.; Pace, T. C. S.; Bohne, C.; Inoue, Y. *Photochem. Photobiol. Sci.* **2010**, *9*, 655−660.
(13) Tamaki, T.; Kokubu, T. *J. Inclusion Phenom.* **1984**, *2*, 815−822.
(14) Tamaki, T.; Kokubu, T.; Ichimura, K. *Tetrahedron* **1987**, *43*, 1485−1494.
(15) Ke, C.; Yang, C.; Mori, T.; Wada, T.; Liu, Y.; Inoue, Y. *Angew. Chem., Int. Ed.* **2009**, *48*, 6675−6677.
(16) Kawanami, Y.; Pace, T. C. S.; Mizoguchi, J.-i.; Yanagi, T.; Nishijima, M.; Mori, T.; Wada, T.; Bohne, C.; Inoue, Y. *J. Org. Chem.* **2009**, *74*, 7908−7921.
(17) Yang, C.; Mori, T.; Inoue, Y. *J. Org. Chem.* **2008**, *73*, 5786−5794.
(18) Ikeda, H.; Nihei, T.; Ueno, A. *J. Org. Chem.* **2005**, *70*, 1237−1242.
(19) Furo, T.; Mori, T.; Wada, T.; Inoue, Y. *J. Am. Chem. Soc.* **2005**, *127*, 8242−8243.
(20) Shibahara, M.; Watanabe, M.; Iwanaga, T.; Matsumoto, T.; Ideta, K.; Shinmyozu, T. *J. Org. Chem.* **2008**, *73*, 4433−4442.
(21) Muranaka, A.; Shibahara, M.; Watanabe, M.; Matsumoto, T.; Shinmyozu, T.; Kobayashi, N. *J. Org. Chem.* **2008**, *73*, 9125−9128.
(22) Harada, N.; Tamai, Y.; Takuma, Y.; Uda, H. *J. Am. Chem. Soc.* **1980**, *102*, 501−506.
(23) Harada, N.; Tamai, Y.; Uda, H. *J. Am. Chem. Soc.* **1980**, *102*, 506−511.
(24) (a) *Time-Dependent Density Functional Theory*; Marques, M. A. L., Ullrich, C. A., Nogueira, F., Rubio, A., Burke, K., Gross, E. K. U., Eds.; Springer-Verlag: Berlin-Heidelberg, Germany, 2006. (b) Casida, M. E. Time-Dependent Density Functional Response Theory for Molecules. In *Recent Advances in Density Functional Methods*; Chong, D. P., Ed.; World Scientific: Singapore, 1995; Vol. *1*, pp 155−192.
(25) For a leading reference on the calculation of the excited states, see : Harbach, P. H. P.; Dreuw, A. The Art of Choosing the Right Quantum Chemical Excited-State Method for Large Molecular Systems. In *Modeling of Molecular Properties*; Comba, P., Ed.; Wiley-VCH: Weinheim, 2011; pp 29−47.
(26) Berova, N.; Nakanishi, K.; Woody, R. W. *Circular Dichroism: Principles and Applications*, 2nd ed.; Wiley: New York, 2000.
(27) Hembury, G. A.; Borovkov, V. V.; Inoue, Y. *Chem. Rev.* **2008**, *108*, 1−73.
(28) Dreuw, A.; Head-Gordon, M. *Chem. Rev.* **2005**, *105*, 4009−4037.
(29) Wang, Y.; Wang, Y.; Wang, J.; Liu, Y.; Yang, Y. *J. Am. Chem. Soc.* **2009**, *131*, 8839−8847.
(30) Bringmann, G.; Gulder, T.; Hertlein, B.; Hemberger, Y.; Meyer, F. *J. Am. Chem. Soc.* **2010**, *132*, 1151−1158.
(31) Diedrich, C.; Grimme, S. *J. Phys. Chem. A* **2003**, *107*, 2524−2539.
(32) Mori, T.; Inoue, Y.; Grimme, S. *J. Phys. Chem. A* **2007**, *111*, 7995−8006.
(33) (a) Tam, M. C.; Abrams, M. L.; Crawford, T. D. *J. Phys. Chem. A* **2007**, *111*, 11232−11241. (b) Kowalczyk, T. D.; Abrams, M. L.; Crawford, T. D. *J. Phys. Chem. A* **2006**, *110*, 7649−7654. (c) Crawford, T. D. *Theor. Chem. Acc.* **2006**, *115*, 227−245. (d) Kongsted, J.; Hansen, A. E.; Pedersen, T. B.; Osted, A.; Mikkelsen, K. V.; Christiansen, O. *Chem. Phys. Lett.* **2004**, *391*, 259−266. (e) Pedersen, T. B.; Koch, H.; Ruud, K. *J. Chem. Phys.* **1999**, *110*, 2883−2892.
(34) Broene, R. D.; Diederich, F. *Tetrahedron Lett.* **1991**, *32*, 5227−5230.
(35) Jones, J. R.; Liotta, C. L.; Collard, D. M.; Schiraldi, D. A. *Macromolecules* **1999**, *32*, 5786−5792.
(36) Platt, J. R. *J. Chem. Phys.* **1949**, *17*, 484−495.
(37) Smith, H. E. *Chem. Rev.* **1998**, *98*, 1709−1740.

(38) Grimme, S.; Antony, J.; Schwabe, T.; Muck-Lhtenfeld, C. *Org. Biomol. Chem.* **2007**, *5*, 741−758.
(39) Grimme, S. *J. Comput. Chem.* **2004**, *25*, 1463−1473.
(40) Grimme, S. *J. Phys. Chem. A* **2005**, *109*, 3067−3077.
(41) Christiansen, O.; Koch, H.; Jorgensen, P. *Chem. Phys. Lett.* **1995**, *243*, 409−418.
(42) Hattig, C.; Kohn, A. *J. Chem. Phys.* **2002**, *117*, 6939−6951.
(43) Pariser, R.; Parr, R. G. *J. Chem. Phys.* **1953**, *21*, 767−776.
(44) Pople, J. A. *Trans. Faraday Soc.* **1953**, *49*, 1375−1385.
(45) Grimme, S. *Rev. Comput. Chem.* **2004**, *20*, 153−218.
(46) Polavarapu, P. L. *Chirality* **2002**, *14*, 768−781.
(47) Goerigk, L.; Grimme, S. *J. Phys. Chem. A* **2009**, *113*, 767−776.
(48) (a) Srebro, M.; Autschbach, J. *J. Chem. Theory Comput.* **2012**, *8*, 245−256. (b) Claps, M.; Parrinello, N.; Saa, C.; Varela, J. A.; Caccamese, S.; Rosini, C. *Tetrahedron: Asymmetry* **2006**, *17*, 1387−1393.
(49) Mewes, J.-M.; Neumann, K.; Verhoefen, M.-K.; Wille, G.; Wachtveitl, J.; Dreuw, A. *ChemPhysChem* **2011**, *12*, 2077−2080.
(50) TURBOMOLE V6.2 2010, a development of University of Karlsruhe and Forschungszentrum Karlsruhe GmbH, 1989−2007, TURBOMOLE GmbH, since 2007; available from http://www.turbomole.com.